



1 **Extrapolating regional probability of drying of headwater streams**
2 **using discrete observations and gauging networks**

3 **Aurélien BEAUFORT**¹, Nicolas LAMOUREUX², Hervé PELLA², Thibault DATRY² and Eric SAUQUET¹

4 ¹Irstea, UR HHLY, Hydrology and Hydraulics Research Unit, 5 rue de la Doua CS 20244, 69625
5 Villeurbanne Cedex, France

6 ²Irstea, UR MALY, Laboratory Dynam, 5 rue de la Doua CS 20244, 69625 Villeurbanne Cedex, France

7 Abstract

Headwater streams represent a substantial proportion of river systems and have frequently flows intermittence due to their upstream position in the network. These intermittent rivers and ephemeral streams have recently seen a marked increase in interest, especially to assess the impact of drying on aquatic ecosystems. The objective of this paper is to quantify how discrete (in space and time) field observations of flow intermittence help to extrapolate the daily probability of drying at the regional scale. Two empirical models based on linear or logistic regressions have been developed to predict the daily probability of intermittence at the regional scale across France. Explanatory variables were derived from available daily discharge and groundwater level data of a dense gauging/piezometer network, and models were calibrated using discrete series of field observations of flow intermittence. The robustness of the models was tested using (1) an independent, dense regional data set of intermittence observations, (2) observations of the year 2017 excluded from the calibration. The resulting models were used to simulate the regional probability of drying in France: (i) over the period 2011-2017 to identify the regions most affected by flow intermittence; (ii) over the period 1989-2017, using a reduced input dataset, to analyze temporal variability of flow intermittence at the national level. The two regressions models performed equally well between 2011 and 2017. The accuracy of predictions depended on the number of continuous gauging/piezometer stations and intermittence observations available to calibrate the regressions.



Regions with the highest performance were located in sedimentary plains, where the monitoring network was dense and where the regional probability of drying was the highest. Conversely, worst performances were obtained in mountainous regions. Finally, temporal projections (1989-2016) suggested highest probabilities of intermittence (> 35%) in 1989-1991, 2003 and 2005. A high density of intermittence observations improved the information provided by gauging stations and piezometers to extrapolate the spatial distribution of intermittent rivers and ephemeral streams.

Keywords: Intermittent rivers, headwater streams, flow regime, discrete observations, regional scale

1. Introduction

Headwater streams represent a substantial proportion of river systems (Leopold et al., 1964; Nadeau and Rains, 2007; Benstead and Leigh, 2012). From an ecological point of view, headwater catchments are at the interface between terrestrial and aquatic ecosystems and they often harbour a unique biodiversity with a very high spatial turn-over (Meyer et al., 2007; Clarke et al., 2008; Finn et al., 2011). Their contribution to the functioning of hydrographic networks is essential: sediment flows, inputs of particulate organic matter and nutrients, refugia/colonization, sources for aquatic organisms (Meyer et al., 2007; Finn et al., 2011).

Headwater streams are generally naturally prone to flow intermittence, i.e. streams which stop flowing or dry up at some point in time and space, mainly due to their upstream position in the network and their high reactivity to natural or human disturbances (Benda et al., 2005; Datry et al., 2014b). These waterways which cease flow and/or dry are referred as intermittent rivers and ephemeral streams (IRES). The geographic extent of IRES is poorly documented due to mapping limitations (digital elevation models, satellite images, aerial photos) and because of their size and their location (Leopold et al., 1994; Nadeau and Rains, 2007; Benstead and Leigh, 2012; Fritz et al., 2013). However the proportion of IRES in hydrological networks can be very large: for example, they represents 60% of the length of rivers in the United States (Nadeau and Rains, 2007) and are



49 considered to represent probably more than 50% of the global hydrological network (Larned et al.,
50 2010; Datry et al., 2014b). Considering only gauging stations with continuous records may lead to
51 severely underestimate their regional extent (Snelder et al., 2013; De Girolamo et al., 2015; Eng et
52 al., 2016).

53 Recently, IRESs have seen a marked increase in interest stimulated by the challenges of water
54 management facing the global change context (water scarcity issues, climate change impact, etc.)
55 (Acuña et al., 2014; Datry et al., 2016b). Studies have characterized the hydrological functioning of
56 IRES (Gallart et al., 2012; Costigan et al., 2016) to assess the effects of flow intermittence on aquatic
57 ecosystems (Larned et al., 2010; Datry et al., 2016b; Leigh et al., 2016; Leigh and Datry, 2017). IRES
58 have been altered due to human actions (abstraction, hill dams, low-water support, pollution, etc.)
59 despite their high and unique biodiversity (Datry et al., 2014; Garcia et al., 2017a). In addition, some
60 perennial streams are becoming intermittent due to global change, water abstraction or river
61 damming (Skoulikidis, 2009) and the extent of IRES may increase in the future (Döll and Schmied,
62 2012; Jaeger et al., 2014; Pumo et al., 2016; Garcia et al., 2017b; De Girolamo et al., 2017).

63 A better hydrological understanding of IRES is now essential and an improved management requires
64 knowing both the spatial extent and arrangement of IRES within the river network (Boulton, 2014;
65 Acuña et al., 2017). Efforts have been made to estimate the spatial distribution of IRES at the
66 catchment scale (Skoulikidis et al., 2011; Datry et al., 2016a), at the regional scale (Gómez et al.,
67 2005) and at the national scale (Snelder et al., 2013). In France, Snelder et al. (2013) suggested a
68 classification of IRES regimes and spatialized their distribution. Based on an analysis of the
69 continuous gauging network, they showed that the proportion of IRES accounted for 20 to 39% of the
70 hydrographic network. The accuracy of the obtained map is highly dependent on the density of the
71 flow monitoring network. The installation of additional gauging stations is expensive and headwaters
72 systems may be difficult to monitor due to active geomorphology processes or to difficult access.



73 As a promising tool to advance the mapping of IRES, citizen science has proved to create
74 opportunities to overcome the lack of hydrological data and lead to densify the flow state
75 observation network (Turner and Richter, 2011; Buytaert et al., 2014; Datry et al., 2016b). In France,
76 Datry et al. (2016a) used such data to describe the spatiotemporal dynamics of aquatic and
77 terrestrial habitats within five river catchments located in the western part of France. They showed
78 that processes resulting in flow intermittence were complex at a fine scale and could vary
79 substantially among nearby catchments. However, these data were only available in few catchments,
80 limiting any attempt to map large-scale patterns of flow intermittence in river networks. Since this
81 first attempt, new sources of observational data have become available in France thanks to the
82 ONDE network (Observatoire National des Etiages, onde.eaufrance.fr). This unique network in
83 Europe provides frequent discrete field observations (five inspections per year) of the flow
84 intermittence across more than 3 300 sites throughout France and located mostly in headwater
85 areas.

86 The objective of this paper is to quantify how discrete (in space and time) field observations of flow
87 intermittence help to extrapolate the daily probability of drying at the regional scale. We first carried
88 out a quantitative analysis of the ONDE network data and to characterize their information
89 contribution in comparison with the data resulting from the conventional hydrological monitoring.
90 Then, two empirical models based on linear or logistic regressions have been developed to convert
91 discontinuous series of flow intermittence observation from ONDE into daily probability of drying at
92 the regional scale across France. Explanatory variables were derived from available daily discharge
93 and groundwater level data of a dense gauging/piezometer network, and models were calibrated
94 using the ONDE discrete observations. The robustness of the models was tested using (1) an
95 independent, dense regional data set of intermittence observations and (2) observations of the year
96 2017 excluded from the calibration. Finally, resulting models were used to simulate the regional
97 probability of drying in France: (i) over the period 2012-2016 to identify the regions most affected by



98 flow intermittence; (ii) over the period 1989-2016, using a reduced input dataset, to analyze
 99 temporal variability of flow intermittence at the national level.

100 **2. Material and Methods**

101 **2.1. Study area**

102 The study area is continental France and Corsica (550 000 km²). France is located in a temperate zone
 103 characterized by a variety of climates due to the influences of the Atlantic Ocean, the Mediterranean
 104 Sea and mountain areas.

105 We defined regions as combinations of "level-2 hydroecoregions" (HER2) and classes of hydrological
 106 regimes (HR). Hydro-EcoRegion (HER) correspond to a typology developed for river management in
 107 accordance with the European Water Framework Directive. The Hydro-ecoregions classification
 108 includes 22 "level-1 hydroecoregions" (HER1) based on geology, topography and climate, and
 109 considered as the primary determinants of the functioning of water ecosystems (Wasson et al.,
 110 2002). HER2 regions correspond to a finer classification accounting for stream size. HER2 have a
 111 mean drainage area of 5 000 km² (between 100 and 27 000 km²). The hydrological regimes classes
 112 (HR) were identified by reference to the work carried out by (Sauquet et al., 2008) where it was
 113 possible to distinguish rainfall-fed regimes, transition and snowmelt-fed river flow regimes. Overall,
 114 we used 280 regions (HER2-HR combinations) with a mean drainage area of 1 400 km² (between 4
 115 and 20 000 km²).

116 **2.2. ONDE dataset discrete national flow-state observations**

117 The ONDE network was set up in 2012 by the French Biodiversity Agency (AFB, formerly ONEMA)
 118 with the aim of constituting a perennial network recording summer low flow levels and used to
 119 anticipate and manage water crisis during severe drought events (Nowak and Durozoi, 2012).



120 There are 3 300 ONDE sites distributed throughout France (Fig. 1). ONDE sites are located on
121 headwater streams with a Strahler order strictly less than 5 and balanced across HER2 regions to take
122 into account the representativeness of the hydrological contexts (Nowak and Durozoi, 2012). The
123 ONDE network is stable over time. Observations are made monthly (around the 25th) by trained AFB
124 staff, between April and September, every year since 2012. One of the statuses is assigned at each
125 observation among “visible flow”, “no visible flow” and “dried out”. Here, we consider two
126 intermittency statuses: “**Flowing**” when there is visible flow across the channel (“visible flow”) and
127 “**Drying**” when the channel is entirely devoid of surface water (“dried out”) or when there is still
128 water in the river bed but without visible flow (disconnected pools, lentic systems) (“no visible
129 flow”). The proportion of drying sites determined on the basis of the ONDE network for each HER2-
130 HR combination is considered as a good estimate of the daily Regional Probability of Drying
131 ($RPoD_{ONDE}$) of streams with a Strahler order less than 5.

132 Figure 2 illustrates the complementary nature of the ONDE network to the already existing French
133 river flow monitoring network HYDRO (<http://www.hydro.eaufrance.fr/>). The ONDE sites and a set of
134 1 600 gauging stations available in the HYDRO database have been projected on the river network
135 RHT (Theoretical Hydrographic Network; Pella *et al.*, 2012) and the drainage area and the elevation
136 have been estimated. A large part of ONDE sites are located on small headwater streams with 70% of
137 the sites with a drainage area of less than 50 km² while most of the gauging stations record flows of
138 catchment of medium size (between 100 and 500 km²). Only four stations display a drainage area of
139 more than 1 000 km². The distributions of elevation of the two databases look similar. The ONDE
140 sites are mostly located on rivers with an elevation below 200 m (75% of sites). The ONDE sites are
141 sparse at high elevations (95 sites located above 1 000 m). The more likely reason of this bias is the
142 difficult access to the river beds in mountainous area.



143 **2.3. POC dataset: a denser regional dataset used for independent** 144 **validation**

145 A spatially denser citizen science dataset of flow-state observations in western France (Poitou-
146 Charente region) (<http://atlas.observatoire-environnement.org>) has been used as validation dataset
147 to test the robustness of our models calibrated with the ONDE dataset. The POC monitoring (2011-
148 2013) covered more than 4 000 km of river length across 20 catchments. Each river was entirely
149 surveyed every 1st and 15th of each month between June and October, resulting in eight observations
150 per year. Four intermittency statuses were available in the POC dataset (Datry *et al.* 2016a) but to
151 allow comparisons with the ONDE network, we pooled the two “Flowing” and “Low Flow” POC
152 statuses into a single “**Flowing**” status and the two “No flow” and “Dry” statuses into the “**Drying**”
153 status. This dataset is available as maps with flow states assigned to the inspected streams. The
154 proportion of drying derived from this dataset for each HER2-HR combination located in the Poitou-
155 Charente region is hereafter called $RPoD_{POC}$.

156 **2.4. Explanatory hydrological dataset**

157 Two hydrological datasets were used as explanatory variables of discrete intermittence observations
158 and for extrapolating the intermittence frequency over time. The two datasets included time series
159 of daily discharge extracted from the French River discharge monitoring network (“HYDRO database”,
160 <http://www.hydro.eaufrance.fr/>): (i) **the 2011-2017 dataset** with full records available between the
161 01/01/2011 and 31/06/2017; (ii) **the 1989-2017 dataset** concerning a reduced number of gauging
162 stations and providing daily discharges between the 01/01/1989 and 31/06/2017. According to the
163 hydrometric services in charge of the selected gauging stations, high quality of measurements was
164 ensured and observed discharges were not or only slightly altered by human actions.

165 The 2011-2017 dataset was composed by 1 600 gauging stations distributed across France. Each
166 stream where a HYDRO gauging station is located has been defined as IRES or perennial. Several
167 definitions of IRES can be found in the literature (Huxter and van Meerveld, 2012, Eng et al., 2016;



168 Reynolds et al., 2015). In this study, we considered stations as intermittent when five consecutive
169 days with discharge less than 1 liter per second has been observed during the period of record.

170 The 1989-2017 dataset consisted of 630 gauging stations selected with less than 5% of missing data
171 (continuous or not) during the period 1989-2017. This dataset has been thereafter used to estimate
172 the proportion of drying before the creation of the ONDE network.

173 **2.5. Explanatory groundwater level dataset**

174 Because groundwater resources influence stream intermittence, we used available time series of the
175 daily groundwater level available in the ADES database (<http://www.adeseaufrance.fr/>) at sites
176 identified as involved in groundwater/surface water exchanges (Brugeron et al., 2012). Similarly to
177 the hydrological data, two sets of groundwater level data with records available over the two periods
178 2011-2017 and 1989-2017 have been selected.

179 The 2011-2017 dataset was composed by 750 piezometers with daily groundwater level data with
180 less than 5% of missing data (continuous or not).

181 The selection of 1989-2017 dataset was not easy because few groundwater level measurements
182 were available in the database before 2000. For example, only five piezometers met the tolerance
183 limit on missing values considered for the 1989-2017 hydrological dataset. In order to extend the
184 dataset and because groundwater levels were less variable than stream discharges, the proportion of
185 permitted gaps was fixed to 20% between 1989 and 2017. This led us to select 150 piezometers.
186 Thereafter, when the missing data period was less than 10 days, groundwater level were
187 reconstructed by linear interpolation in order to reduce the proportion of missing values to less than
188 5% for the 150 piezometers selected.

189 **2.6. Statistical modeling of regional probability of drying**

190 A regional probability of drying (RPoD) was calculated on each sampling date and for each HER2-HR
191 combination. The parametric modeling strategy was based on 4 main steps (Fig. 3). The first step



consisted in selecting all ONDE sites, gauging stations and piezometers located in a same HER2-HR combination. When the total number of gauging stations and piezometers was less than 5 for a HER2-HR combination, we merged 20 of the 280 regions with a neighboring one located in the same HER1. The second step consisted in calculating the $RPoD_{ONDE}$ for each observation date (5 per year) and for all selected ONDE sites. In a third step, a flow duration curve was determined for each selected HYDRO gauging station. The average non-exceedance frequency of the observed discharge at gauging stations was calculated between the date of observation (d) at ONDE sites and the 5 days preceding the observation. The lag of six days accounted for the fact that ONDE survey dates in a region could differ by 5 days, and accounted for the inertia of physical processes (e.g. storage capacity); it was chosen after a few trials. The same operation was carried out with selected piezometers. Finally the hydrological conditions are described by the weighted average F of the non-exceedance frequencies of discharge and groundwater levels with respect to the relative proportions of gauging stations and piezometers.

The fourth step consisted in estimating the $RPoD_{ONDE}$ as a function of F. Two types of regression were fitted for each HER2-HR combination across France:

a truncated logarithmic linear regression (LLR), with two parameters α_1 and β_1 :

$$RPoD_{LLR} = \begin{cases} \min(1; \alpha_1 \times \ln(F) + \beta_1) & \text{when } F < F0 \\ 0 & \text{when } F \geq F0 \end{cases} \quad (1)$$

$F0$ was fixed as the value of non-exceedance frequencies of discharge and groundwater levels at which no more drying was observed across the ONDE network ($RPoD_{ONDE} = 0$).

a logistic regression (LR), with two parameters α_2 and β_2 :

$$\text{Logit}(RPoD_{LR}) = \ln\left(\frac{RPoD_{LR}}{1-RPoD_{LR}}\right) = \alpha_2 \times F + \beta_2 \quad (2)$$

LR is a multivariate analysis method well known for its relevance in binary classification issues (Lee, 2005). The $RPoD_{LR}$ was then calculated as following Eq. 3:



$$\text{RPoD}_{LR} = \frac{\exp(\alpha_2 + \beta_2 F)}{1 + \exp(\alpha_2 + \beta_2 F)} \quad (3)$$

2.7. Model robustness: validation using independent data sets

We used the POC independent data and the 2017 ONDE year to test the robustness of the LLR and LR model to predict the intermittence frequency in space and time. Note that when predicting on the POC datasets, a new model was calibrated using only ONDE sites located out of POC streams.

For both datasets (POC and ONDE 2017), the relative performance of the LLR and LR models was compared in multiple ways using both the 2011-2017 and the 1989-2017 datasets. The performance of each model was evaluated by the Nash-Sutcliffe efficiency criterion (NSE) (Nash and Sutcliffe, 1970):

$$NSE = 1 - \frac{\sum_{i=1}^N (\text{RPoD}_{\text{ONDE}i} - \text{RPoD}_{\text{pri}})^2}{\sum_{i=1}^N (\text{RPoD}_{\text{ONDE}i} - \overline{\text{RPoD}_{\text{ONDE}}})^2} \quad (4)$$

where $\text{RPoD}_{\text{ONDE}i}$ is the average proportion of drying over the ONDE sites located in the HER2-HR combination at the i^{th} observation date, RPoD_{pri} is the predicted regional probability of drying at the i^{th} observation date, $\overline{\text{RPoD}_{\text{ONDE}}}$ is the mean of $\text{RPoD}_{\text{ONDE}i}$ over the period and N is the total number of observations in the ONDE network for each HER2-HR combination.

2.8. Model prediction

Both models have been calibrating over the period 2012-2016 and were then applied in a 5th step to predict the daily RPoD in France (Fig. 3). The RPoD was firstly predicted over the period 2012-2016 in order to identify the most affected regions by flow intermittence using the 2011-2017 datasets. The second application concerned the prediction of RPoD in France over a longer period using the 1989-2017 dataset to analyze the temporal variability of flow intermittence at the national level. It should



235 be noted that models predictions only concern streams with a Strahler order lower than 5 due to the
 236 ONDE sites location.

237 **3. Results**

238 **3.1. Quantitative analysis**

239 **3.1.1. Inter-annual intermittence analysis with the ONDE network**

240 A total of 1 127 ONDE sites have recorded at least one drying during the period 2012-2016
 241 representing 35% of the 3 300 ONDE sites. Between 2012 and 2016, the most critical year is 2012
 242 with 15% of drying followed by 2016 (14%) and 2015 (14%) (Fig. 4a). The year 2013 and 2014 are less
 243 affected with only 6% of drying observed (Fig. 4a).

244 Drying mainly occur between July and September but the evolution of the month's proportion of
 245 drying can differ between years (Fig. 4). In more details, water levels in 2012 decrease in August
 246 when the proportion of drying is 27% and the situation lasts until the end of September with 25% of
 247 drying (Fig. 4b). In 2013, the drying proportion is lower than in 2012 but follow the same pattern with
 248 an increased at the end of July (3%) and reached 9% in August and in September. In 2014, the first
 249 peak of drying (5%) is reached early in June. Then, the drying proportion decreases in July (3%) and
 250 increases slightly in August 4% and reach 7% in September. In 2015, the critical period occur at the
 251 end of July with 19% of drying and the proportion of drying decreases slightly at the end of August
 252 (17%) until reaching 9% in September. Finally, in 2016, the situation is gradually deteriorated every
 253 month, reaching 20% of drying in August, and 28% in September.

254 Between 2012 and 2016, a proportion of drying higher than 50% is recorded on 93 ONDE sites and
 255 their spatial distribution is very patchy at the France scale (black and dark grey dots, Fig. 5a). There
 256 are only 158 ONDE sites with at least one drying every year and a variability of drying locations can
 257 be observed across years. The south-east of France is heavily affected by rivers drying where drying
 258 proportion can exceed 75% annually (black dots, Fig. 5b-5f). The north-western part of France is less



259 affected, although many ONDE sites show a drying proportion observed above 50% in 2014 and 2016
260 (Fig. 5d and 5f). Northeastern France is rather affected in 2012, 2014 and 2015 where several ONDE
261 sites have more than 75% of drying (Fig. 5b, 5d and 5e). The south-west France is particularly
262 affected in 2012 and 2015 (Fig. 5b and 5e).

263 3.1.2. Comparison of flow intermittence between ONDE network and HYDRO dataset

264 HYDRO dataset includes 90 gauging stations located on streams considered as IRES, which represents
265 only 5.5% of the 3 300 gauging stations against 35% for ONDE sites. At the national scale, the number
266 of IRES seems underrepresented in the south-western, central, northeastern part of France and
267 Corsica in comparison with sites experiencing drying in the ONDE network (Fig. 6).

268 The number of gauging stations with at least one drying (discharge < 1 l/s) observed between May
269 and September varies between 79 in 2012 and 47 in 2014 (Table 1). The lowest numbers of gauging
270 stations with drying are observed in the years 2013 and 2014 while the highest numbers are related
271 to the years 2012, 2015 and 2016. This finding is consistent with the analysis of the ONDE network
272 (Fig. 5a, d). The frequency of drying calculated between the 1st May and 30st September, in contrast,
273 is quite constant over the years (~30%). The number of gauging stations with drying over more than
274 50% of the time varies little between wet years (14 in 2013) and dry years (21 in 2015) unlike ONDE
275 observations which suggest a significant temporal variability in the frequency of drying between dry
276 and wet years (Fig. 5).

277 3.2. Validation of the predicted regional probability of drying

278 3.2.1. Regression results

279 LLR and LR models, calibrated over the period 2012-2016, perform well with the 2011-2017 dataset
280 with a mean NSE of 0.8 with LR model against 0.7 with LLR model (Fig. 7a and b). With the LR model,
281 50% of the HER2-HR combinations obtain a NSE greater than 0.8, representing a coverage of 65% of
282 the French territory, while 33% of HER2-HR combinations display a NSE higher than 0.8 (50% of
283 France coverage) with the LLR model. Regions with the highest performances are located in



284 sedimentary plains, in the south-east of France and in the Pyrenees Mountains. Conversely, the
285 worst performances are obtained in the mountainous regions of Alps as well as in the Massif Central.
286 In these regions the size of the HER2 is rather small and the number of ONDE sites, gauging stations
287 and piezometers per HER2-HR combinations are certainly too few to derive reliable relations. Despite
288 pooling, estimating RPOD remains impossible for 9 HER2-HR combinations (4.5% of France coverage)
289 because the number of ONDE sites, gauging stations and piezometers sites is insufficient (less than 5)
290 to perform the regression analysis.

291 The performance level is lower when the 1989-2017 dataset is used in models: the mean NSE with
292 the LR and LLR models is 0.7 and 0.6, respectively (Fig. 7c and d).

293 The LR and LLR models lead to similar performance range. However, the LR model outperforms the
294 LLR model in terms of number of HER2-HR combinations with NSE greater than 0.8 (Fig. 7c and d).
295 The performance is sensitive to the dataset. As expected, the best results are obtained with the
296 denser network. A decrease in NSE by more than 0.2 is identified for 5% of the French territory when
297 the 1989-2017 dataset is used (black areas; Fig. 7e and f). The regions with the most degraded values
298 of NSE are small HER2-HR combinations located in eastern France (Fig. 7e and f).

299 The decrease in performance is mainly due to the difference in number of gauging stations and
300 piezometers between the two datasets (Fig. 8). The most degraded NSEs correspond to HER2-HR
301 combinations where the number of gauging stations and piezometers considered in regressions is
302 the most reduced, i.e. with a loss higher than 50% of stations (black and dark grey dots; Fig 8a and b).
303 However, the decrease in performance remains low (difference in NSE is below 0.1 for 75% and 64%
304 of HER2-HR combinations with LLR and LR model, respectively).

305 **3.2.2. Comparison to the POC database**

306 The observed proportion of drying RPOD_{POC} is rather well simulated by both LLR and LR models with
307 the 2011-2017 dataset (NSE > 0.7 except for the year 2011, Fig. 10). In addition, the models are able
308 to capture small fluctuations of RPOD_{POC} during the summer period. The best results during the year



2011 are obtained with the LLR model (black curve; Fig. 9) and the LR model overestimates $RPoD_{POC}$ by 3% (dashed grey curve; Fig. 9). In 2012, the decline in water levels is more gradual than in 2011 and a marked peak is reached in September with 40% of $RPoD_{POC}$ (Fig. 9). This pattern is well reproduced by both models with a good fit to all observation points (Fig. 9). The year 2013 is less affected by drying occurrence and the maximum $RPoD_{POC}$ does not exceed 20% (Fig. 9). Curves of both models fit to observations well until the end of August. Note that the LR model is slightly closer to the observations around the peak in September compared to the LLR model. However the LR model overestimates the $RPoD_{POC}$ at the end of September and in October.

The simulations of $RPoD$ are weakly degraded when both models use with the 1989-2017 dataset (Fig. 9d, e, f). However the simulated pattern is similar to the observed one. The LLR model outperforms the LR model during the three years of validation with the 1989-2017 dataset (black curve; Fig. 9d, e, f).

3.2.3. Temporal patterns assessment of models between 2012 and 2017

The LLR and LR models perform similarly whatever the dataset (with an average NSE of 0.7 between 2012 and 2017 with the two datasets, Tab. 2). Note that both models tend to better simulate the $RPoD$ during dry years 2012 and 2016 (NSE = 0.8 with LLR and LR models; Tab. 2) than during wet years (e.g. 2014 with NSE < 0.7).

Less satisfactory performance is achieved for the two months in the year 2017 (NSE < 0.5). Figure 10 shows the dispersion between simulated $RPoD$ and drying observed at ONDE sites in the scatter plot leading to a R^2 of 0.53 with the LLR model and 0.45 with the LR model. The lower performance in the year 2017 may be explained by an earlier drying conditions (June) compared with the previous years with a dry season between August and September. However, both models seem able to predict $RPoD$ out of the calibration period.

332



3.3. Application of regional models

3.3.1. Modeling of intermittencies severity between 2012 and 2016

Both models have been applied using the 2011-2017 dataset. Figure 11 displays the maximum number of consecutive days ($D_{\text{RPoD}>20\%}$) with RPoD higher than 20% simulated by both LLR and LR models. The most affected regions are located in the south-east of France and in sedimentary plains which are consistent with the spatial pattern obtained from the ONDE observations (Fig. 5). The most impacted year followed the same hierarchy: the year 2012 is the most critical year with 30% of France displaying $D_{\text{RPoD}>20\%}$ higher than 60 days followed by the year 2015 (20% of France with $D_{\text{RPoD}>20\%} > 60$ days) and 2016 (15% of France with $D_{\text{RPoD}>20\%} > 60$ days) (Fig. 11). The years 2013 and 2014 are weakly affected with 5% and 6% of the France with $D_{\text{RPoD}>20\%}$ higher than 60 days, respectively.

The LR model tends to simulate shorter periods of drying, particularly in HER2-HR combinations located in the South-East France in 2013 and 2014 (Fig. 11). However, there is an overall agreement between RPoD simulated by both models in terms of spatial and temporal extension of dry streams.

3.3.2. Reconstitution of historical regional probability of drying

The trend temporal patterns of RPoD predicted by the two models, considering the 1989-2017 dataset, look similar between 1989 and 2016 and the simulated RPoD fit well to $\text{RPoD}_{\text{ONDE}}$ (Fig. 12). The results confirm the ability to reproduce the current conditions with both models, as discussed previously (Tab. 2).

The proportion of drying is highly variable over the total simulation period, with alternating dry (1989 to 1991, 2003 to 2006, 2009 to 2012) and wet (1994 to 1995, 2000 to 2002; 2013 to 2014) phases. In spite of interannual variability, peaks of RPoD occur regularly between August and September, whether in dry years or wet years. This finding is consistent with the preeminence of rainfall fed river flow regime with low flows in summer, in France.



357 The highest values of RPoDs (above 35% over France) are observed in 1989, 1990, 1991, 2003 and
358 2005 (black curve, Fig. 12a and b). The RPoDs simulated during these dry years are out of the range
359 of the observed values over the calibration period (2012-2016). Estimations are thus uncertain.
360 However, the high values of RPoD are consistent with observations reported in previous studies (e.g.
361 Larue and Giret, 2004; Snelder et al., 2013; Caillouet et al., 2017). Conversely, the years less affected
362 by drying are simulated in 1994, 2001 and 2014 with an average RPoD below 15% throughout the
363 year (black curve, Figs. 12a and b).

364 Results obtained with the LLR model are more contrasted in terms of extreme values than those
365 obtained with the LR model (Fig. 12b).

366 4. Discussion

367 *ONDE network complementarity with conventional flow monitoring network*

368 The analysis of the ONDE observations shows that the proportion of rivers undergoing drying is
369 significantly higher (35%) than that observe with the conventional monitoring (HYDRO database, 8%).
370 This proportion although related to a short period of records 2012 and 2016 is consistent with the
371 percentage of 39% of river segments classified as intermittent by Snelder at al. (2013). This analysis
372 confirms the under-representation of IRES in the French HYDRO database. Without any information
373 on headwater, Snelder et al. (2013) were unable to predict IRES in eastern France (see Fig. 9, pp.
374 2694). The high density of ONDE sites makes it possible to improve the dryings detection and lead to
375 better capture spatial distribution of IRES located at the upstream the hydrographic network. The
376 ONDE network encompasses various hydrological conditions which provides a more accurate
377 assessment of inter-annual variability, differentiating between dry years (2012, 2015 and 2016) and
378 wet years (2013, 2014) with clearly few drying occurrences.

379 The validation of the LR and LLR models against the POC database demonstrates also the
380 representativeness of the ONDE network. Thanks to the qualitative information provided and to



381 models such as statistical models developed here, it is now possible to capture drying event at the
382 regional scale.

383 The ONDE sites are located on small headwater streams which can be very reactive to external
384 disturbances (rainfall deficit, change in air temperature, increase in water withdrawals, etc.) and by
385 nature are more likely to be IRES. The gauging stations available in the HYDRO database are located
386 on larger streams and their hydrologic response to changes in external factors (environmental or
387 human) is slower and drying occurred with greater inertia under temperate climate. Their uneven
388 distribution across France does not allow to accurately characterize the inter-annual variability of
389 drying development.

390 ONDE network provides very complementary information to conventional flow monitoring, leading
391 to a better understanding of the processes of drying in upstream catchments.

392 *Dependency on spatial gauging networks density*

393 The performance obtained with the LR and LLR models is slightly better with the 2011-2017 dataset
394 (mean NSE ~ 0.75) than those obtained with the 1989-2017 dataset (mean NSE > 0.65), whose
395 network is less dense. HER2-HR combinations are the most degraded where the number of
396 monitoring stations is the most decreased between the two datasets. The accuracy of the predictions
397 is dependent on the number of gauging stations, ONDE sites and piezometers available to calibrate
398 the regressions. Highest NSEs are obtained in western sedimentary plains and southeastern of France
399 where a significant number of streams have dryings regardless of years (Fig. 5). The dominant river
400 flow regime in these regions is mainly influenced by precipitation and the lowest water levels are
401 reached in August and September, which corresponds to the monitoring period of the ONDE
402 database. They benefit from a dense monitoring network (gauging stations, ONDE sites,
403 piezometers), which allows a better representation of the hydrological functioning of streams
404 located within the same HER2. Conversely, performance was poor in mountainous areas such as in
405 the Alps or the Massif Central (NSE < 0.4) where river flow regimes are diversified combining rainfall



406 and snowmelt influences. By construction, the area of HER2-HR combination in mountains is
407 reduced, which leads to a limited number of monitoring stations, certainly not sufficient to fit the
408 models. Moreover, the observation period for ONDE sites was limited between May and September
409 and dryings can be missed, particularly for streams influenced by snow or glaciers melting with low
410 flows in winter.

411 We have chosen to average the non-exceedance frequencies of flows and groundwater levels in
412 order to increase the monitoring network. If models have been calibrated using only gauging
413 stations, performance will have been globally similar, or slightly better, in some HER2-HR
414 combinations (Fig. 13). There is thus no conclusion on a possible bias due to the use of piezometers.
415 This is certainly due to the dominant proportion of the gauging stations compared to the
416 piezometers. Indeed, in the 2011-2017 dataset, the proportion of gauging stations is greater than
417 75% for more than 70% of HER2-HR combinations whereas the proportion of piezometers exceeds
418 70% in only 5% of HER2-HR combinations. Groundwater level data thus have small weight in
419 regressions for this dataset. However, in the 1989-2017 dataset, the proportion of piezometer is
420 greater than 70% in more than 30% of HER2-HR combinations. The presence of piezometers
421 increases the density of the monitoring network in HER2-HR combinations with few available gauging
422 stations. Thanks to groundwater level data, RPoD can be predicted on more HER2-HR combinations.

423 *Interest in reconstructing the dynamic regional probability of drying*

424 Spatio-temporal simulation of the probability of drying is crucial for advancing our understanding of
425 IRES ecology and management. Some aquatic species can persist in dry reach for a few days, weeks
426 or months, while some are highly sensitive to desiccation (Datry, 2012; Storey and Quinn, 2013;
427 Stubbington and Datry, 2013). Estimating the total duration of the drying at the reach scale is
428 therefore needed to understand biological patterns in river networks. In France, based on the 2011-
429 2017 dataset, both models suggest highest values of RPoD along the Mediterranean coast
430 ($D_{RPoD>20\%} > 100$ days each year). Rivers in this region are subject to a predominantly pluvial regime



431 (Class 7; Sauquet et al., 2008), i.e. hot and dry summers follow by intense rainfall events in autumn,
432 leading to high flows in November (Skoulikidis et al., 2017b). The catchments in this region are small
433 and particularly reactive to environmental changes, making them highly sensitive to flow
434 intermittence. Rivers located in sedimentary plain in western France are also very impacted by flow
435 intermittence. The regime is also influenced by precipitation and the basins are subject of intense
436 agriculture with important water withdrawals during summer. Abstractions greatly reduce the water
437 availability in rivers and in aquifers which are no longer able to support the low water levels and lead
438 to increased flow intermittence. The responses of biological communities to artificial flow
439 intermittence is still poorly understood compared to natural IRES (Datry et al., 2014b, Skoulikidis et
440 al., 2017a).

441 *Validity of historical regional probability of drying during severe low-flow period*

442 The second application aimed at reconstructing historical RPoD over the period 1989-2016. Both
443 models suggest highest values of mean RPoD (> 35%) in 1989-1991, 2003 and 2005. During these dry
444 years, predicted values of RPoD results from extrapolation but are consistent with published studies
445 (Mérillon and Chaperon, 1990, Moreau, 2004). For example, Mérillon (1992) estimated that for the
446 whole of France, 11 000 km of rivers were dried at the end of summers of 1989 and 1990. Caillouet
447 et al (2016) found that the low-flow event observed in 1989-1990 was particularly severe in terms of
448 duration and affected 95% France territory. Snelder et al. (2013) showed from 628 gauging stations
449 that the years 1989-1991, 2003 and 2005 had witnessed particularly high values of duration and
450 frequency of drying. They found that regions with the highest probability of drying were located
451 along the Mediterranean and Atlantic coasts, which is consistent with ONDE observations and with
452 our results.

453 Both models suggest the same sequence of dry and wet years. However the application of the LLR
454 model lead to less contrasted RPoD than LR model (Fig. 12).



455 To illustrate these differences, the RPoD has been simulated by both models with a fictive extreme F
456 of 1% (Fig. 14). The RPoD_{LLR} is significantly higher and exceeds 80% in 30% of the France territory
457 against only 5% of the territory with the RPoD_{LR} . On the other hand, models simulate low RPoD in
458 HER2-HR combinations where the $\text{RPoD}_{\text{ONDE}}$ is very low between 2012-2016, even when F was 1%
459 because this situation never occurred during the calibration period (Fig. 14). The logistic function of
460 the LR model takes an S-shape which induced a crushing of extreme values around the maximal
461 values observed during the calibration period (2012-2016). The truncated logarithmic function of the
462 LLR model is not bounded and RPoD can reach 100% during extreme low flow events by
463 extrapolation. ONDE network has not witnessed a severe low-flow period as in 1990. In that sense, it
464 is not currently possible to differentiate between the two models similar performances over the
465 same calibration period. Refining extrapolated values require additional information on headwater
466 collected during more severe droughts than those observed during the last five years and then gives
467 support to the pursuit of the ONDE network.

468 5. Conclusion

469 This paper investigates the spatial and temporal dynamics of the regional probability of drying (RPoD)
470 of headwater streams by taking benefit from qualitative and discontinuous data provided by the
471 ONDE network. Two models based on linear or logistic regressions have been used to reconstruct the
472 temporal dynamics of RPoD. They are based on a strong relationship between the non-exceedance
473 frequencies of discharges and groundwater levels as a function of the proportion of drying observed
474 at ONDE sites per HER2-HR combination. LLR and LR models show similar performance and perform
475 well between 2011 and 2017. The accuracy of predictions is dependent on the number of gauging
476 stations, ONDE sites and piezometers available to calibrate the regressions. Regions with the highest
477 performance are located in sedimentary plains, where the monitoring network is dense and where
478 the RPoD is the highest. Conversely, the worst performances are obtained in the mountainous
479 regions. Finally, both models have been used to reconstitute historical RPoD between 1989 and 2016



480 and suggest highest values of mean RPoD ($> 35\%$) in 1989-1991, 2003 and 2005. This is consistent
481 with other published studies but the high density of ONDE sites makes it possible to improve the
482 dryings detection and lead to better capture the spatial distribution of IRES located at the upstream
483 the hydrographic network.

484 The next step will be to use this regional approach to simulate the RPoD in future periods by taking
485 into account effects of climate change through predicted discharge and groundwater level data. This
486 would allow to quantify the evolution of the probability of drying between the current period and
487 the different climate projections provided by the latest IPCC Report (IPCC 2014a, 2014b) report and
488 would assist decision makers in defining protocols for restoring flows with appropriate measures to
489 preserve aquatic ecosystems (Woelfle-Erskine, 2017).

490 Secondly, further work is needed to develop an approach capable of reconstructing the drying
491 dynamics locally by differentiating each stream. This will allow decision makers to take more
492 appropriate measures to limit locally and more effectively the IRES development and thus preserve
493 the biodiversity of these environments. Our approach remains spatially valid to estimate RPoDs at
494 the scale of HER2-HR combinations and does not allow characterizing the variability of the probability
495 of drying occurrence between nearby streams within these regions. However, previous studies have
496 shown that this could be very complex because diverse flow states (lentic, lotic, flowing) could
497 develop in the same segment of river separated by small distances and create highly fragmented
498 hydrographic networks (Datry et al., 2016a). It is necessary to take into account many drivers
499 involved in the flow intermittence development such as: rainfall, potential evapotranspiration, air
500 temperature, exchanges between open channels and groundwater systems, riparian vegetation,
501 water abstraction, river bed topography, etc. These variables are rarely available at fine scales at a
502 country scale. From a methodological point of view, statistical tools such as neural networks
503 (Breiman, 2001) have shown good ability to assess both the occurrence and extent of perennial and



504 temporary segments (González-Ferreras and Barquín, 2017) and could be investigated as an
505 alternative method to reconstruct locally the temporal variability of drying.

506 **6. Acknowledgment**

507 The research project was partly funded by the French Agency for Biodiversity (AFB, formerly
508 ONEMA). This study is based upon works from COST Action CA15113 (SMIRES, Science and
509 Management of Intermittent Rivers and Ephemeral Streams, www.smires.eu), supported by COST
510 (European Cooperation in Science and Technology).



7. References

- Acuña, V., Datry, T., Marshall, J., Barceló, D., Dahm, C. N., Ginebreda, A., McGregor, G., Sabater, S., Tockner, K. and Palmer, M. A.: Why should we care about temporary waterways?, *Science*, 343(6175), 1080–1081, 2014.
- Acuña, V., Hunter, M. and Ruhí, A.: Managing temporary streams and rivers as unique rather than second-class ecosystems, *Biological Conservation*, 211, 12–19, doi:10.1016/j.biocon.2016.12.025, 2017.
- Benda, L., Hassan, M. A., Church, M. and May, C. L.: Geomorphology Of Steepland Headwaters: The Transition From Hillslopes To Channels¹, *Journal of the American Water Resources Association*, 41(4), 835, 2005.
- Benstead, J. P. and Leigh, D. S.: An expanded role for river networks, *Nature Geoscience*, 5(10), 678–679, 2012.
- Boulton, A. J.: Conservation of ephemeral streams and their ecosystem services: what are we missing?: Editorial, *Aquatic Conservation: Marine and Freshwater Ecosystems*, 24(6), 733–738, doi:10.1002/aqc.2537, 2014.
- Breiman, L.: Random forests, *Machine learning*, 45(1), 5–32, 2001.
- Buytaert, W., Zulkafli, Z., Grainger, S., Acosta, L., Alemie, T. C., Bastiaensen, J., De Bièvre, B., Bhusal, J., Clark, J., Dewulf, A., Foggin, M., Hannah, D. M., Hergarten, C., Isaeva, A., Karpouzoglou, T., Pandeya, B., Paudel, D., Sharma, K., Steenhuis, T., Tilahun, S., Van Hecken, G. and Zhumanova, M.: Citizen science in hydrology and water resources: opportunities for knowledge generation, ecosystem service management, and sustainable development, *Frontiers in Earth Science*, 2, doi:10.3389/feart.2014.00026, 2014.
- Clarke, A., Mac Nally, R., Bond, N. and Lake, P. S.: Macroinvertebrate diversity in headwater streams: a review, *Freshwater Biology*, 53(9), 1707–1721, doi:10.1111/j.1365-2427.2008.02041.x, 2008.
- Costigan, K. H., Jaeger, K. L., Goss, C. W., Fritz, K. M. and Goebel, P. C.: Understanding controls on flow permanence in intermittent rivers to aid ecological research: integrating meteorology, geology and land cover: Integrating Science to Understand Flow Intermittence, *Ecohydrology*, 9(7), 1141–1153, doi:10.1002/eco.1712, 2016.
- Datry, T.: Benthic and hyporheic invertebrate assemblages along a flow intermittence gradient: effects of duration of dry events: River drying and temporary river invertebrates, *Freshwater Biology*, 57(3), 563–574, doi:10.1111/j.1365-2427.2011.02725.x, 2012.
- Datry, T., Larned, S. T., Fritz, K. M., Bogan, M. T., Wood, P. J., Meyer, E. I. and Santos, A. N.: Broad-scale patterns of invertebrate richness and community composition in temporary rivers: effects of flow intermittence, *Ecography*, 37(1), 94–104, doi:10.1111/j.1600-0587.2013.00287.x, 2014a.
- Datry, T., Larned, S. T. and Tockner, K.: Intermittent Rivers: A Challenge for Freshwater Ecology, *BioScience*, 64(3), 229–235, doi:10.1093/biosci/bit027, 2014b.
- Datry, T., Pella, H., Leigh, C., Bonada, N. and Hugueny, B.: A landscape approach to advance intermittent river ecology, *Freshwater Biology*, 61(8), 1200–1213, doi:10.1111/fwb.12645, 2016a.



- 549 Datry, T., Fritz, K. and Leigh, C.: Challenges, developments and perspectives in intermittent river
550 ecology, *Freshwater Biology*, 61(8), 1171–1180, doi:10.1111/fwb.12789, 2016b.
- 551 De Girolamo, A. M., Lo Porto, A., Pappagallo, G., Tzoraki, O. and Gallart, F.: The Hydrological Status
552 Concept: Application at a Temporary River (Candelaro, Italy): EVALUATING HYDROLOGICAL STATUS
553 IN TEMPORARY RIVERS, *River Research and Applications*, 31(7), 892–903, doi:10.1002/rra.2786,
554 2015.
- 555 De Girolamo, A. M., Bouraoui, F., Buffagni, A., Pappagallo, G. and Lo Porto, A.: Hydrology under
556 climate change in a temporary river system: Potential impact on water balance and flow regime,
557 *River Research and Applications*, doi:10.1002/rra.3165, 2017.
- 558 Döll, P. and Schmied, H. M.: How is the impact of climate change on river flow regimes related to the
559 impact on mean annual runoff? A global-scale analysis, *Environmental Research Letters*, 7(1),
560 014037, doi:10.1088/1748-9326/7/1/014037, 2012.
- 561 Eng, K., Wolock, D. M. and Dettinger, M. D.: Sensitivity of Intermittent Streams to Climate Variations
562 in the USA: Sensitivity of Intermittent Streams, *River Research and Applications*, 32(5), 885–895,
563 doi:10.1002/rra.2939, 2016.
- 564 Finn, D. S., Bonada, N., M?rria, C. and Hughes, J. M.: Small but mighty: headwaters are vital to stream
565 network biodiversity at two levels of organization, *Journal of the North American Benthological*
566 *Society*, 30(4), 963–980, doi:10.1899/11-012.1, 2011.
- 567 Fritz, K. M., Hagenbuch, E., D’Amico, E., Reif, M., Wigington, P. J., Leibowitz, S. G., Comeleo, R. L.,
568 Ebersole, J. L. and Nadeau, T.-L.: Comparing the Extent and Permanence of Headwater Streams From
569 Two Field Surveys to Values From Hydrographic Databases and Maps, *JAWRA Journal of the*
570 *American Water Resources Association*, 49(4), 867–882, doi:10.1111/jawr.12040, 2013.
- 571 Gallart, F., Prat, N., García-Roger, E. M., Latron, J., Rieradevall, M., Llorens, P., Barberá, G. G., Brito,
572 D., De Girolamo, A. M., Lo Porto, A., Buffagni, A., Erba, S., Neves, R., Nikolaidis, N. P., Perrin, J. L.,
573 Querner, E. P., Quiñonero, J. M., Tournoud, M. G., Tzoraki, O., Skoulidakis, N., Gómez, R., Sánchez-
574 Montoya, M. M. and Froebrich, J.: A novel approach to analysing the regimes of temporary streams
575 in relation to their controls on the composition and structure of aquatic biota, *Hydrology and Earth*
576 *System Sciences*, 16(9), 3165–3182, doi:10.5194/hess-16-3165-2012, 2012.
- 577 Garcia, C., Gibbins, C. N., Pardo, I. and Batalla, R. J.: Long term flow change threatens invertebrate
578 diversity in temporary streams: Evidence from an island, *Science of The Total Environment*, 580,
579 1453–1459, doi:10.1016/j.scitotenv.2016.12.119, 2017a.
- 580 Garcia, C., Amengual, A., Homar, V. and Zamora, A.: Losing water in temporary streams on a
581 Mediterranean island: Effects of climate and land-cover changes, *Global and Planetary Change*, 148,
582 139–152, doi:10.1016/j.gloplacha.2016.11.010, 2017b.
- 583 González-Ferreras, A. M. and Barquín, J.: Mapping the temporary and perennial character of whole
584 river networks: MAPPING FLOW PERMANENCE IN RIVER NETWORK, *Water Resources Research*,
585 doi:10.1002/2017WR020390, 2017.
- 586 Huxter, E. H. H. and (Ilja) van Meerveld, H. J.: Intermittent and Perennial Streamflow Regime
587 Characteristics in the Okanagan, *Canadian Water Resources Journal / Revue canadienne des*
588 *ressources hydriques*, 37(4), 391–414, doi:10.4296/cwrj2012-910, 2012.



- 589 Jaeger, K. L., Olden, J. D. and Pelland, N. A.: Climate change poised to threaten hydrologic
590 connectivity and endemic fishes in dryland streams, *Proceedings of the National Academy of*
591 *Sciences*, 111(38), 13894–13899, doi:10.1073/pnas.1320890111, 2014.
- 592 Larned, S. T., Datry, T., Arscott, D. B. and Tockner, K.: Emerging concepts in temporary-river ecology,
593 *Freshwater Biology*, 55(4), 717–738, doi:10.1111/j.1365-2427.2009.02322.x, 2010.
- 594 Lee, S.: Application of logistic regression model and its validation for landslide susceptibility mapping
595 using GIS and remote sensing data, *International Journal of Remote Sensing*, 26(7), 1477–1491,
596 doi:10.1080/01431160412331331012, 2005.
- 597 Leigh, C. and Datry, T.: Drying as a primary hydrological determinant of biodiversity in river systems:
598 a broad-scale analysis, *Ecography*, 40(4), 487–499, doi:10.1111/ecog.02230, 2017.
- 599 Leigh, C., Boulton, A. J., Courtwright, J. L., Fritz, K., May, C. L., Walker, R. H. and Datry, T.: Ecological
600 research and management of intermittent rivers: an historical review and future directions,
601 *Freshwater Biology*, 61(8), 1181–1199, doi:10.1111/fwb.12646, 2016.
- 602 Meyer, J. L., Strayer, D. L., Wallace, J. B., Eggert, S. L., Helfman, G. S. and Leonard, N. E.: The
603 Contribution of Headwater Streams to Biodiversity in River Networks¹: The Contribution of
604 Headwater Streams to Biodiversity in River Networks, *JAWRA Journal of the American Water*
605 *Resources Association*, 43(1), 86–103, doi:10.1111/j.1752-1688.2007.00008.x, 2007.
- 606 Nadeau, T.-L. and Rains, M. C.: Hydrological Connectivity Between Headwater Streams and
607 Downstream Waters: How Science Can Inform Policy¹: Hydrological Connectivity Between
608 Headwater Streams and Downstream Waters: How Science Can Inform Policy, *JAWRA Journal of the*
609 *American Water Resources Association*, 43(1), 118–133, doi:10.1111/j.1752-1688.2007.00010.x,
610 2007.
- 611 Nash, J. E. and Sutcliffe, J. V.: River flow forecasting through conceptual models part I — A discussion
612 of principles, *Journal of Hydrology*, 10(3), 282–290, doi:10.1016/0022-1694(70)90255-6, 1970.
- 613 Nowak, C. and Durozoi, B.: Observatoire National Des Etiages, Note technique, ONEMA., 2012.
- 614 Pella, H., Lejot, J., Lamouroux, N. and Snelder, T.: Le réseau hydrographique théorique (RHT) français
615 et ses attributs environnementaux, *Géomorphologie: relief, processus, environnement*, 18(3), 317–
616 336, 2012.
- 617 Pumo, D., Caracciolo, D., Viola, F. and Noto, L. V.: Climate change effects on the hydrological regime
618 of small non-perennial river basins, *Science of The Total Environment*, 542, 76–92,
619 doi:10.1016/j.scitotenv.2015.10.109, 2016.
- 620 Reynolds, L. V., Shafroth, P. B. and LeRoy Poff, N.: Modeled intermittency risk for small streams in the
621 Upper Colorado River Basin under climate change, *Journal of Hydrology*, 523, 768–780,
622 doi:10.1016/j.jhydrol.2015.02.025, 2015.
- 623 Sauquet, E., Gottschalk, L. and Krasovskaia, I.: Estimating mean monthly runoff at ungauged
624 locations: an application to France, *Hydrology Research*, 39(5–6), 403, doi:10.2166/nh.2008.331,
625 2008.
- 626 Skoulikidis, N. T.: The environmental state of rivers in the Balkans—A review within the DPSIR
627 framework, *Science of The Total Environment*, 407(8), 2501–2516,
628 doi:10.1016/j.scitotenv.2009.01.026, 2009.



- 629 Skoulidakis, N. T., Vardakas, L., Karaouzas, I., Economou, A. N., Dimitriou, E. and Zogaris, S.: Assessing
630 water stress in Mediterranean lotic systems: insights from an artificially intermittent river in Greece,
631 *Aquatic Sciences*, 73(4), 581–597, doi:10.1007/s00027-011-0228-1, 2011.
- 632 Skoulidakis, N. T., Vardakas, L., Amaxidis, Y. and Michalopoulos, P.: Biogeochemical processes
633 controlling aquatic quality during drying and rewetting events in a Mediterranean non-perennial river
634 reach, *Science of The Total Environment*, 575, 378–389, doi:10.1016/j.scitotenv.2016.10.015, 2017a.
- 635 Skoulidakis, N. T., Sabater, S., Datry, T., Morais, M. M., Buffagni, A., Dörflinger, G., Zogaris, S., del Mar
636 Sánchez-Montoya, M., Bonada, N., Kalogianni, E., Rosado, J., Vardakas, L., De Girolamo, A. M. and
637 Tockner, K.: Non-perennial Mediterranean rivers in Europe: Status, pressures, and challenges for
638 research and management, *Science of The Total Environment*, 577, 1–18,
639 doi:10.1016/j.scitotenv.2016.10.147, 2017b.
- 640 Snelder, T. H., Datry, T., Lamouroux, N., Larned, S. T., Sauquet, E., Pella, H. and Catalogne, C.:
641 Regionalization of patterns of flow intermittence from gauging station records, *Hydrology and Earth
642 System Sciences*, 17(7), 2685–2699, doi:10.5194/hess-17-2685-2013, 2013.
- 643 Storey, R. G. and Quinn, J. M.: Survival of aquatic invertebrates in dry bed sediments of intermittent
644 streams: temperature tolerances and implications for riparian management, *Freshwater Science*,
645 32(1), 250–266, doi:10.1899/12-008.1, 2013.
- 646 Stubbington, R. and Datry, T.: The macroinvertebrate seedbank promotes community persistence in
647 temporary rivers across climate zones, *Freshwater Biology*, 58(6), 1202–1220,
648 doi:10.1111/fwb.12121, 2013.
- 649 Turner, D. S. and Richter, H. E.: Wet/Dry Mapping: Using Citizen Scientists to Monitor the Extent of
650 Perennial Surface Flow in Dryland Regions, *Environmental Management*, 47(3), 497–505,
651 doi:10.1007/s00267-010-9607-y, 2011.
- 652 Wasson, J.-G., Chandesris, A., Pella, H. and Blanc, L.: Typology and reference conditions for surface
653 water bodies in France: the hydro-ecoregion approach, *TemaNord*, 566, 37–41, 2002.
- 654 Woelfle-Erskine, C.: Collaborative Approaches to Flow Restoration in Intermittent Salmon-Bearing
655 Streams: Salmon Creek, CA, USA, *Water*, 9(3), 217, doi:10.3390/w9030217, 2017.
- 656
- 657



658

	Stations with at least one drying event	Stations with drying > 50%	Frequency of discharge < 1 l/s
2012	79	19	32.7
2013	47	14	37.9
2014	54	15	32.9
2015	76	21	31.1
2016	71	19	28.6

Table 1. Annual statistics on flow intermittence calculated on HYDRO gauging stations between the
 1st May and the 30th September

661



		2011-2017 dataset						1989-2017 dataset					
		2012	2013	2014	2015	2016	2017	2012	2013	2014	2015	2016	2017
LLR model	May	0.2	0.0	0.5	0.5	0.6	0.4	0.2	0.0	0.3	0.0	0.7	0.2
	June	0.6	0.3	0.8	0.5	0.8	0.5	0.6	0.3	0.5	0.3	0.8	0.5
	July	0.7	0.5	0.6	0.6	0.8		0.7	0.5	0.5	0.4	0.8	
	August	0.8	0.6	0.7	0.7	0.8		0.7	0.5	0.5	0.5	0.8	
	Sept.	0.7	0.8	0.6	0.6	0.7		0.6	0.7	0.5	0.5	0.6	
	May - Sept	0.8	0.8	0.7	0.7	0.8	0.5	0.8	0.7	0.5	0.6	0.8	0.5
LR model	May	0.2	0.0	0.5	0.1	0.6	0.3	0.3	0.0	0.3	0.0	0.7	0.2
	June	0.6	0.5	0.8	0.5	0.8	0.4	0.6	0.4	0.5	0.3	0.7	0.4
	July	0.7	0.6	0.5	0.6	0.8		0.7	0.4	0.5	0.4	0.8	
	August	0.7	0.6	0.7	0.6	0.7		0.6	0.4	0.5	0.4	0.7	
	Sept.	0.6	0.8	0.6	0.7	0.7		0.5	0.6	0.4	0.5	0.6	
	May - Sept	0.8	0.8	0.7	0.7	0.8	0.4	0.8	0.7	0.5	0.6	0.8	0.4

Table 2. NSE criteria obtained between 2012 and 2017 with the LLR and LR models calibrated over the period 2012-2016.

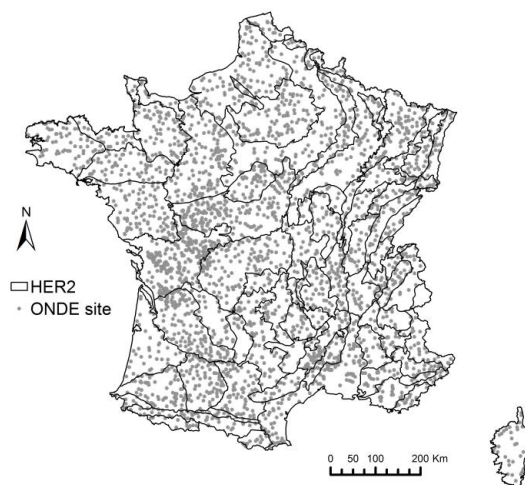


Figure 1. Location of the 3 300 ONDE sites and partition into HER2.

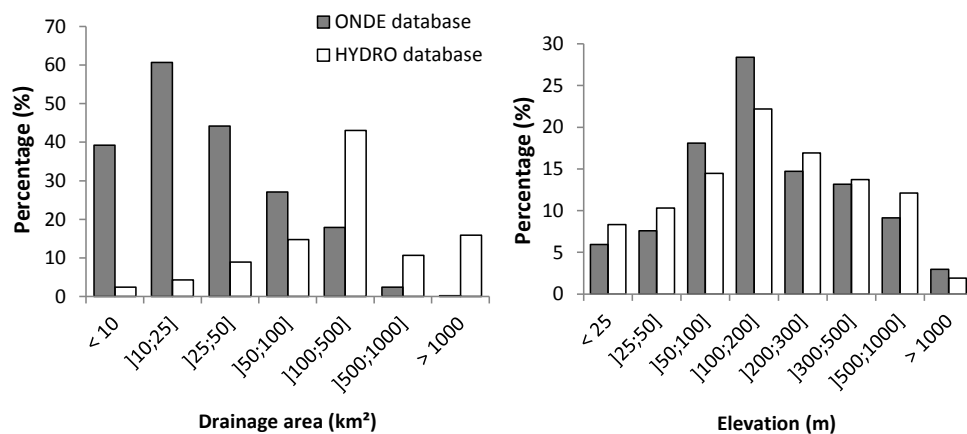


Figure 2. Distribution of the 3 300 ONDE sites and of the 1 600 gauging stations available in the HYDRO database against: (a) drainage area and (b) elevation.

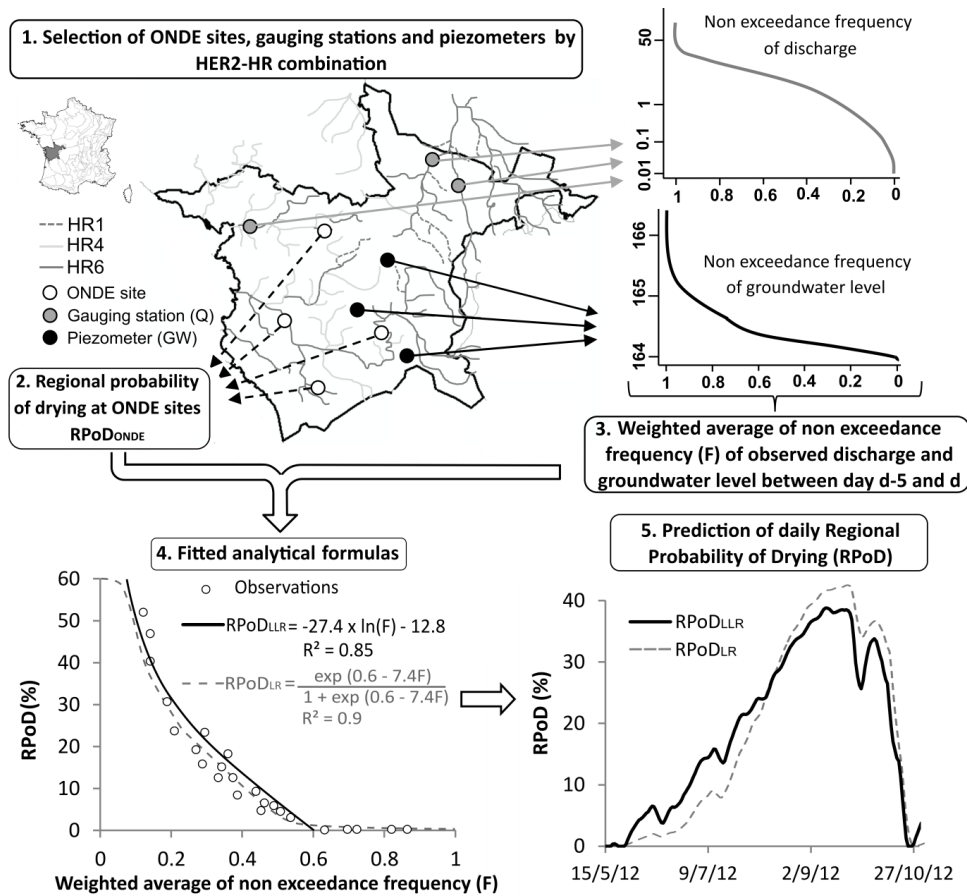


Figure 3. Strategy of parametric modeling (step 1-4) developed to predict (step 5) the regional probability of drying (RPoD) by HER2-HR combination in France.

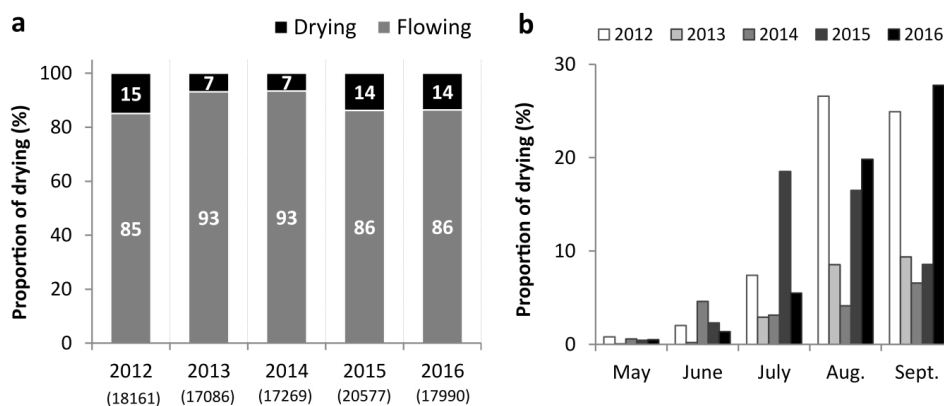


Figure 4. (a) Distribution of yearly proportion of drying observed with the ONDE network with the total yearly number of ONDE observations written in brackets and (b) distribution of proportions of drying per year and per month.

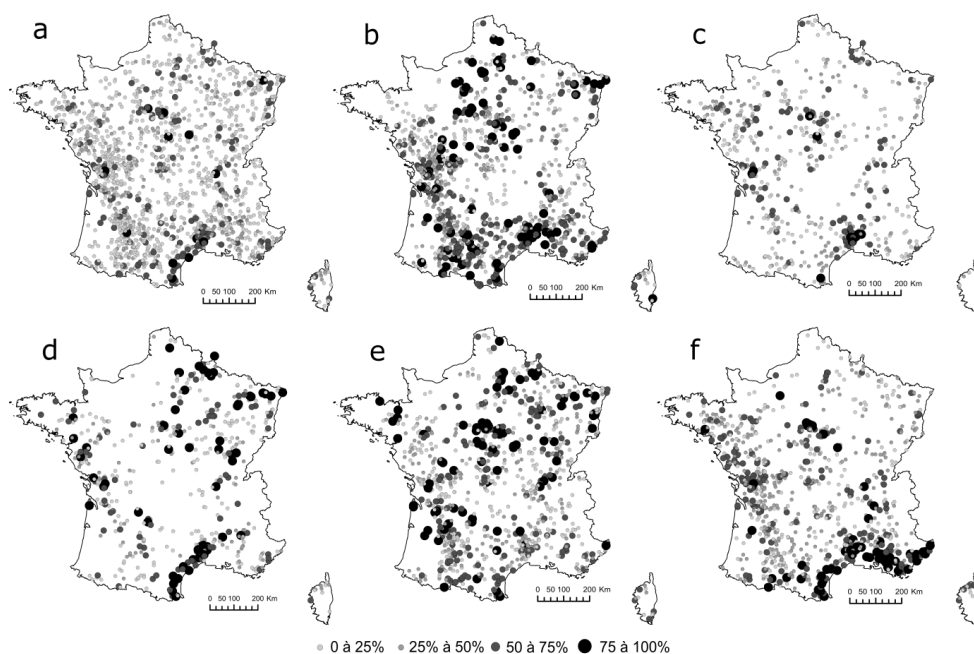


Figure 5. Distribution of the percentages of drying observed at ONDE sites for the years: (a) 2012-2016, (b) 2012, (c) 2013, (d) 2014, (e) 2015 and (f) 2016.

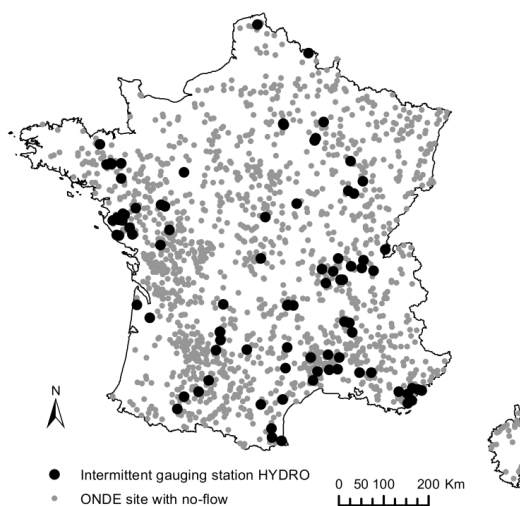
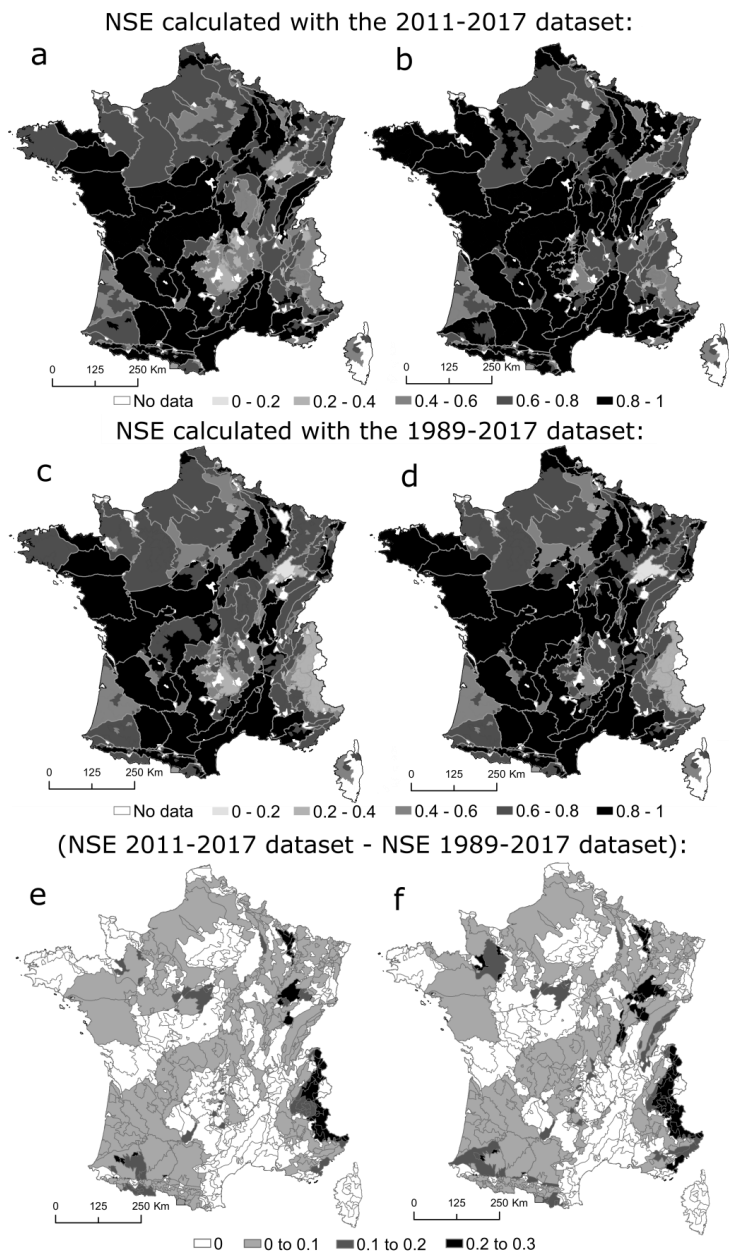


Figure 6. Map of ONDE sites and HYDRO gauging stations having at least one drying.



688

689 **Figure 7.** Map of Nash-Sutcliffe criteria (NSE) obtained for each HER2-HR combination between 2012
690 and 2016 with the 2011-2017 and 1989-2017 datasets according to: (a) and (c) a log-linear regression
691 (LLR) model; (b) and (d) a logistic regression (LR) model. NSE differences between the 2011-2017
692 dataset and the 1989-2017 dataset are represented for: (e) LLR model and (f) LR model.

693

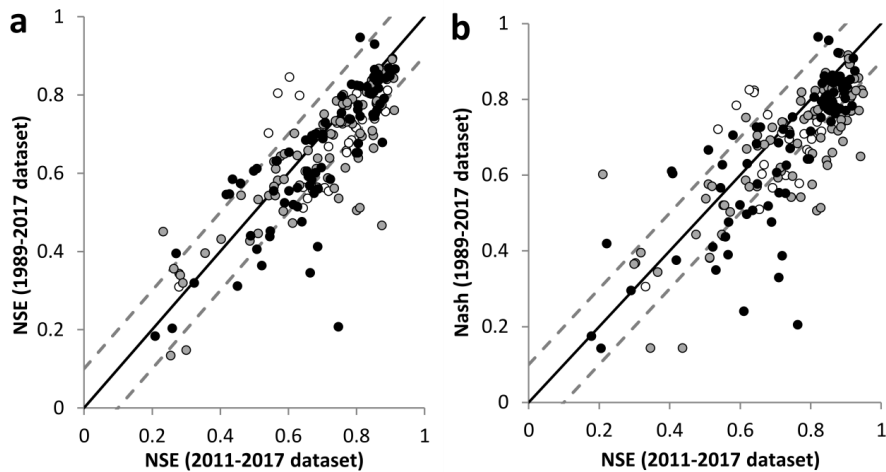
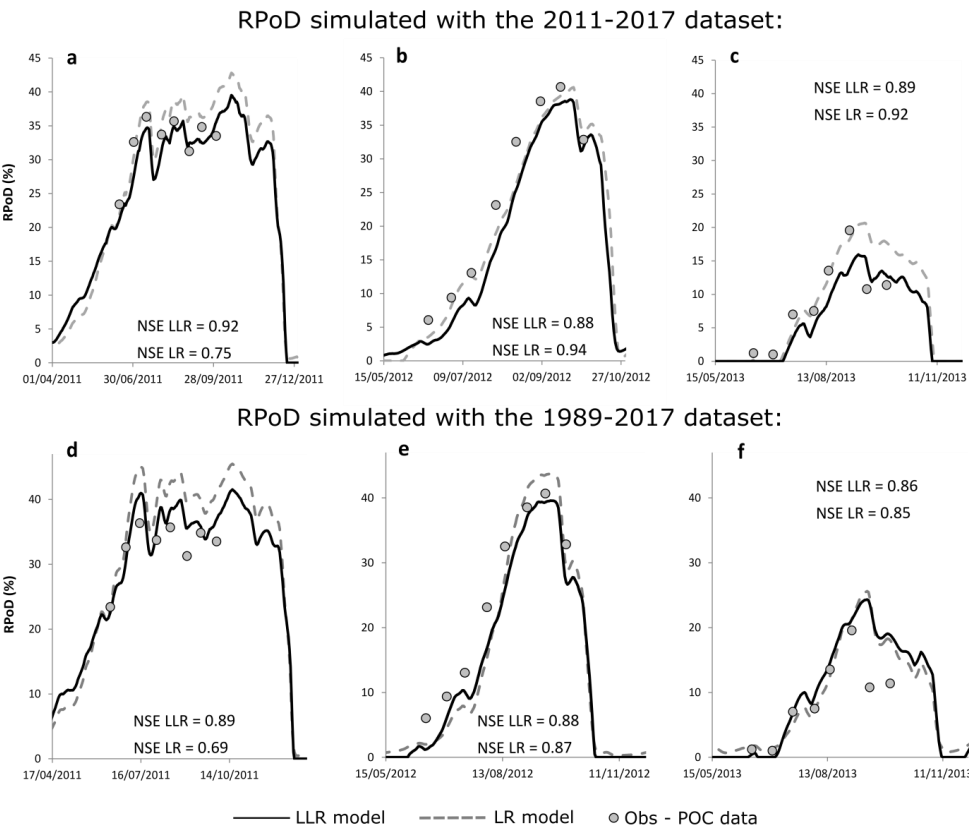


Figure 8. Nash-Sutcliffe criteria (NSE) calculated for each HER2-HR combination between 2012 and 2016 with the 1989-2017 dataset as a function of NSE calculated with 2011-2017 dataset with respectively: (a) the LLR model and (b) the LR model. The color of dots represents the proportion of gauging station and piezometers lost between the 2011-2017 database and the 1989-2017 database: losses < 50% (white); losses between 50% and 75% (grey); losses > 75% (black).



701

702 **Figure 9.** Comparison between observed proportion of drying $RPOD_{POC}$ and $RPOD$ predicted by the LLR
703 and LR models with the 2011-2017 dataset in: (a) 2011, (b) 2012 (c) 2013 and with the 1989-2017
704 dataset in: (d) 2011, (e) 2012 (f) 2013.

705

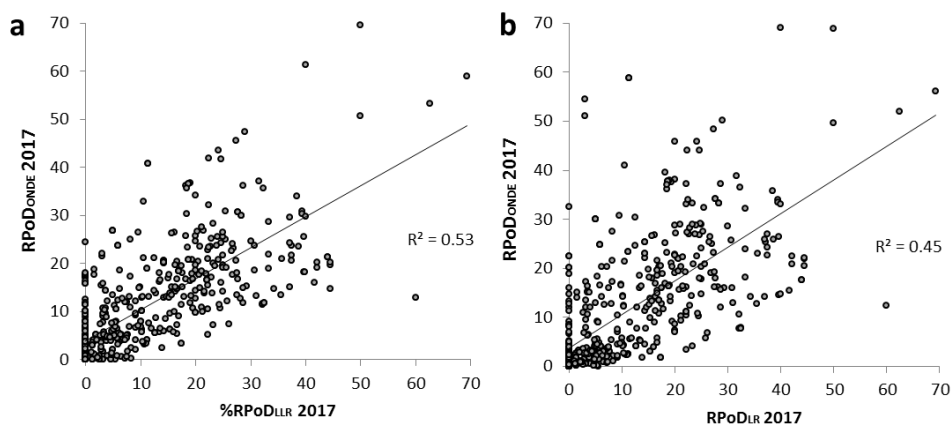


Figure 10. Scatter plot of the predicted RPoD (x axis) and drying observed at ONDE sites (y axis) in 2017 simulated with the 2011-2017 dataset by: (a) the LLR model and (b) the LR model.

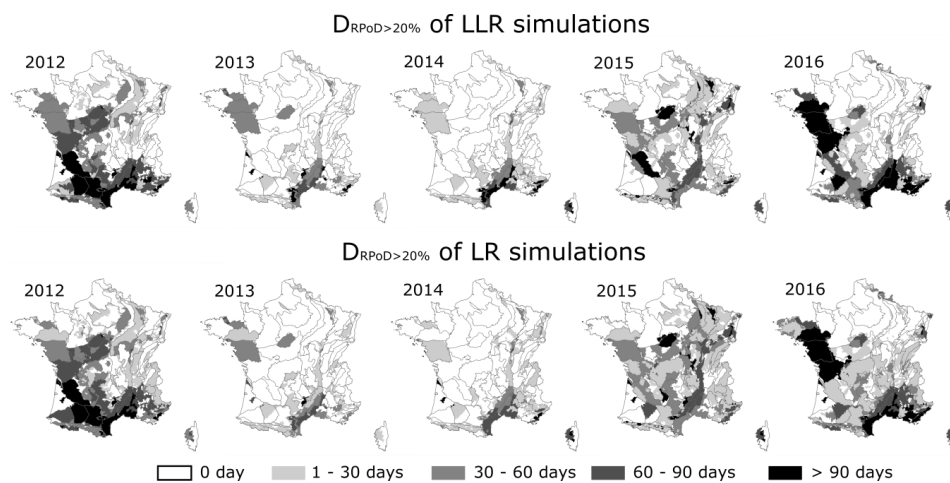


Figure 11. Maximum duration of consecutive days with RPoD higher than 20% simulated with LLR and LR model.

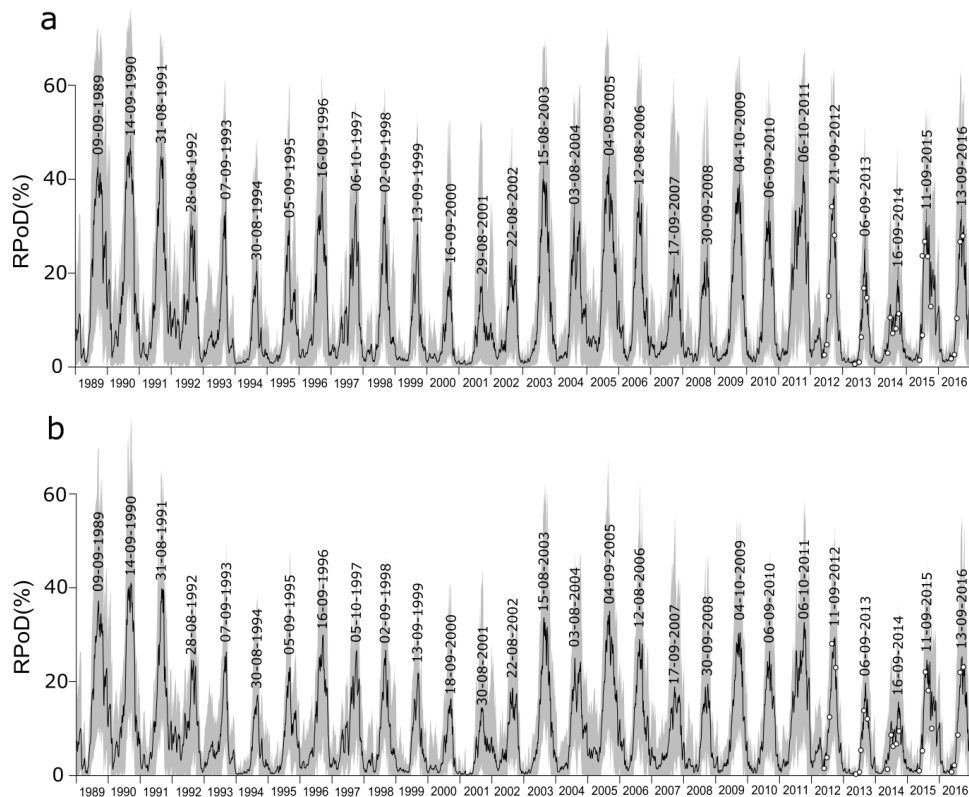


Figure 12. RPOD simulated between 1989 and 2016 with: (a) the LR model and (b) the LLR model. The grey area represents the RPOD between the 90th percentile and the 10th percentile simulated on HER2-HR combination, the black curve represents the average RPOD simulated by HER2-HR combination and white dots represent the mean RPOD_{ONDE} for each observation dates.

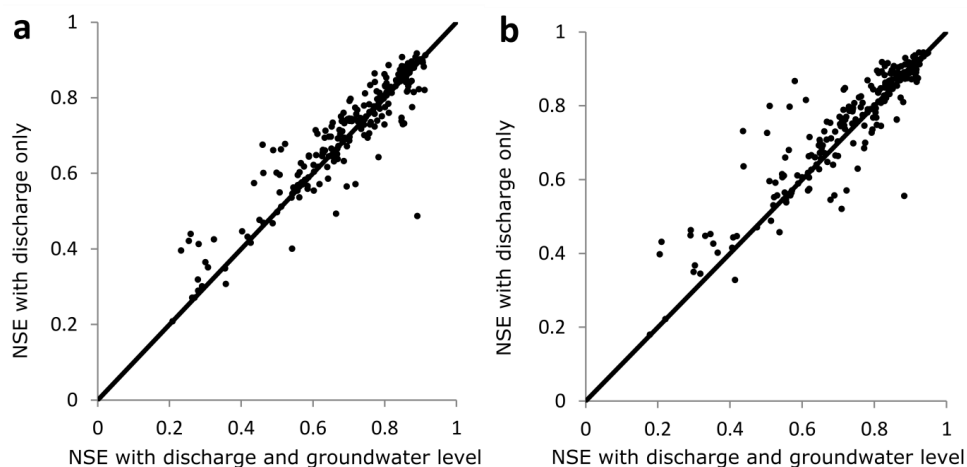


Figure 13. Comparison of NSE obtained with regression including only discharge variable as a function of NSE obtained with including discharge and groundwater level variables in the 2011-2017 dataset with: (a) LLR model and (b) LR model.

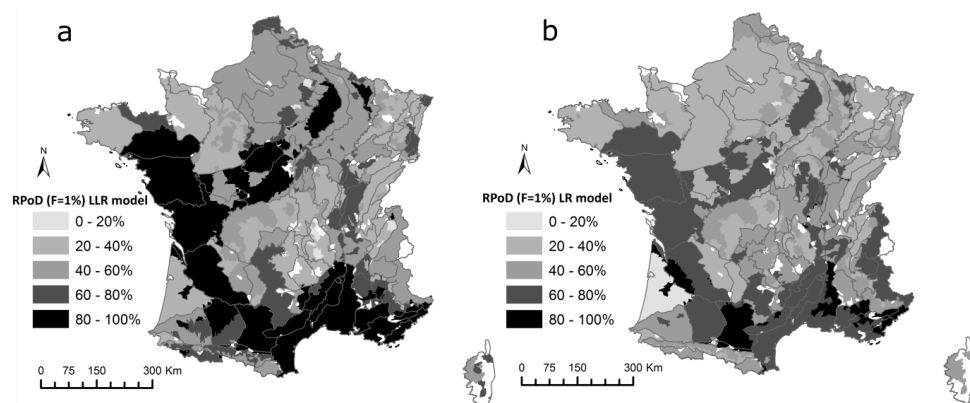


Figure 14. Regional probability of drying simulated with $F = 1\%$ predicted with: (a) the LLR model and (b) the LR model.